Cell PRESS
Neuron
Article

Retrograde BMP Signaling Controls Synaptic Growth at the NMJ by Regulating Trio Expression in Motor Neurons

Robin W. Ball,[1,2] Maude Warren-Paquin,[1,2] Kazuya Tsurudome,[1] Edward H. Liao,[1] Fatima Elazzouzi,[1] Chelsea Cavanagh,[1] Beum-Soo An,[1] Tian-Tian Wang,[1] John H. White,[1] and A. Pejmun Haghighi[1,*]
[1]Department of Physiology, McGill University, Montréal, QC H3G 1Y6, Canada
[2]These authors contributed equally to this work
*Correspondence: pejmun.haghighi@mcgill.ca
DOI 10.1016/j.neuron.2010.04.011

SUMMARY

Retrograde signaling is essential for coordinating the growth of synaptic structures; however, it is not clear how it can lead to modulation of cytoskeletal dynamics and structural changes at presynaptic terminals. We show that loss of retrograde bone morphogenic protein (BMP) signaling at the *Drosophila* larval neuromuscular junction (NMJ) leads to a significant reduction in levels of Rac GEF Trio and a diminution of transcription at the *trio* locus. We further find that Trio is required in motor neurons for normal structural growth. Finally, we show that transgenic expression of Trio in motor neurons can partially restore NMJ defects in larvae mutant for BMP signaling. Based on our findings, we propose a model in which a retrograde BMP signal from the muscle modulates GTPase activity through transcriptional regulation of Rac GEF *trio*, thereby regulating the homeostasis of synaptic growth at the NMJ.

INTRODUCTION

Structural and functional synaptic plasticity are fundamental features of the developing and adult nervous systems, required for establishing neuronal circuits and tuning brain activity. While a multitude of extracellular growth-promoting signals have been implicated in the regulation of synaptic plasticity, we know little about the processes through which these signals can result in changes in the morphology and growth of synaptic structures. In recent years, a growing body of evidence has highlighted the importance of retrograde signaling mechanisms that orchestrate the coordinated growth of pre- and postsynaptic structures (Davis, 2006; Fitzsimonds and Poo, 1998; Regehr et al., 2009). Perhaps one of the best in vivo characterized retrograde mechanisms is a bone morphogenic protein (BMP) signaling cascade responsible for maintaining normal synaptic growth at the *Drosophila* neuromuscular junction (NMJ), where the signal initiated in the postsynaptic muscle by the BMP ligand Glass bottom boat (Gbb) induces receptor activity in presynaptic motor neurons culminating in the increased phosphorylation of the BMP transcription factor, Mothers against dpp (Mad), and its consequent accumulation in the nucleus (Aberle et al., 2002; Marqués et al., 2002; McCabe et al., 2003). Loss or disruption in this signaling cascade at either the level of ligand, receptor or transcription factors leads to a severe reduction in the growth of synaptic boutons at the NMJ (Aberle et al., 2002; Keshishian and Kim, 2004; Marqués et al., 2002; McCabe et al., 2003, 2004). The general consensus is that this Smad-dependent BMP signaling acts as a transcriptional regulator; however, no target genes relevant to synaptic growth have been identified to date.

Modulation of actin cytoskeletal dynamics is often a critical converging point in the induction of synaptic remodeling (Cingolani and Goda, 2008; Luo, 2002; Matus et al., 2000). Among a myriad of molecules that have been shown to interact with the actin cytoskeleton are members of the Rho family of small GTPases: Rho, Rac, and Cdc42. These molecular switches act as major intracellular regulators of the actin cytoskeleton in many cells, including neurons (de Curtis, 2008). In particular, Rac appears to have a prominent role in instructing axonal growth, branching and guidance, as well as in the induction of dendritic growth and spine formation (Dickson, 2001; Luo, 2000, 2002; O'Donnell et al., 2009; Van Aelst and Cline, 2004). Similarly, the upstream activators of Rho-GTPases, guanine exchange factors (GEFs), have been implicated in activity-dependent and activity-independent changes in postsynaptic structural modification (Bryan et al., 2004; Fu et al., 2007; Ma et al., 2003). Little is known, however, about the role of GEFs in regulating the growth of presynaptic structures following the initial formation of synaptic connections.

We show that both wild-type Rac and a GEF-independent form of Rac can induce significant synaptic overgrowth at the NMJ when overexpressed in the motor neurons of *Drosophila* larvae. Interestingly, we find that the action of wild-type but not that of the GEF-independent Rac requires BMP signaling. We demonstrate that retrograde BMP signaling at the NMJ directly regulates the transcription of *trio* gene, a GEF that is required for Rac activation. Consistent with the role of BMP signaling in the regulation of synaptic growth, we find that loss of *trio* leads to a significant reduction in NMJ growth, which is restored by providing Trio in presynaptic neurons. Finally, we show that transgenic expression of Trio in motor neurons can partially

rescue the structural defects at the NMJ in *Mad* and *wit* mutant larvae. Our findings suggest that the regulation of NMJ growth by BMP signaling is, at least in part, achieved through the regulation of *trio* transcription and thereby modulation of Rac GTPase activity.

RESULTS

BMP Signaling Is Required for Rac-Induced NMJ Overgrowth

Synaptic boutons at the *Drosophila* larval NMJ undergo tremendous growth during larval development to keep pace with the fast growing postsynaptic muscles (Schuster et al., 1996). A retrograde BMP signaling cascade plays a central role in maintaining this homeostatic synaptic growth during larval development (Keshishian and Kim, 2004; McCabe et al., 2003, 2004); however, we know little about the molecular links between the retrograde signal and the cytoskeletal rearrangements that allow for NMJ growth. The Rho family of GTPases have been shown to respond to extracellular signals during axon guidance and growth, as well as for the generation and motility of postsynaptic spines (Lai and Ip, 2009; Van Aelst and Cline, 2004; Watabe-Uchida et al., 2006; Yang and Bashaw, 2006); thus, we probed for possible links between BMP signaling and Rho GTPase activity in *Drosophila* larval NMJ development.

As a first step, we tested whether changes in the activity of Rho GTPases in motor neurons can influence presynaptic growth during larval development. We took advantage of the Gal4-UAS system (Brand and Perrimon, 1993) and overexpressed either Rho or Rac specifically in motor neurons using BG380-Gal4 (Budnik et al., 1996). There are three highly homologous Rac genes in the *Drosophila* genome: Rac1, Rac2, and Mtl; we have focused our study on Rac1. We examined the number of boutons per muscle surface area (MSA) in wandering third instar larvae using pre- and postsynaptic markers. We found that overexpression of Rac or a constitutively active form of Rac (Rac-V12), but not that of constitutively active Rho (Rho-V14) led to NMJ overgrowth during larval development (see Figure S1 available online and Figure 1), resulting in an increase in the number of synaptic boutons, branches and the appearance of abnormal structures we call synaptic protrusions (Figures 1 and S1). We also tested larvae carrying two transgenic copies of Cdc42 expressed under the control of the ubiquitin promoter (Rodal et al., 2008) but did not detect any changes in NMJ growth (Figure S1C). The Rac-induced overgrowth was seen with other neuronal Gal4 drivers (OK6-Gal4 and elav-Gal4), but not when Rac was overexpressed in muscle using MHC-Gal4 (Figure S1E).

As Rac activity is known to influence axon growth and guidance during embryonic development (Hakeda-Suzuki et al., 2002; Ng et al., 2002), we wanted to determine whether the enhancement in NMJ growth required Rac during embryonic stages. We tested the effect of Rac activation temporally using elav-GeneSwitch-Gal4 (elav-GS), which is a neuronal Gal4 inducible in the presence of the synthetic steroid hormone RU486 (Osterwalder et al., 2001). Using a Myc-tagged Rac transgene we determined that in the absence of RU486 there was no detectable expression of Rac-Myc, but when larvae were grown on RU486-containing food, Rac-Myc was expressed at the NMJ (Figures S1H–S1N). We found that overexpression of Rac during larval stages only was sufficient to cause synaptic overgrowth (Figures S1H–S1N). Together, the above results suggest that Rac GTPase activity during larval development can influence NMJ growth.

Next, we asked whether Rac-induced enhancement of NMJ growth depended on the presence of intact BMP signaling in motor neurons. We examined the consequence of loss of BMP signaling and found that loss of *Mad* or the BMP type II receptor *wishful thinking* (*wit*) led to a strong suppression of Rac-induced synaptic growth (Figures 1A–1E; $p < 0.0001$ for suppression by *Mad* or *wit*). These results suggested that Rac in motor neurons is dependent on BMP signaling for its ability to induce synaptic growth. To rule out a direct effect on Rac expression in *Mad* and *wit* mutants, we measured the levels of endogenous Rac protein in wild-type larvae and larvae mutant for the BMP ligand *gbb*, *Mad*, the BMP transcriptional cofactor *Medea* (*Med*), and *wit* and found similar Rac protein expression in all (Figure 1F). In addition, we overexpressed Rac-Myc in motor neurons and found that Rac can localize in axons and at synaptic boutons in *Mad* mutants as it does in wild-type larvae (Figures 1G–1J). These results ruled out any direct effect of BMP signaling on Rac expression in motor neurons.

Small GTPases are molecular switches that alternate between active GTP-bound and inactive GDP-bound states. The GDP-GTP conformational change is mediated by guanine nucleotide exchange factors (GEFs) (Bos et al., 2007). To explore a potential link between BMP signaling and Rac activation, we tested whether loss of *Mad* can also suppress NMJ overgrowth in response to overexpression of the constitutively active, GEF-independent Rac-V12. In contrast to the strong effects observed on Rac-induced overgrowth, loss of *Mad* or *wit* did not lead to any significant suppression of NMJ overgrowth when Rac-V12 was overexpressed in motor neurons (Figures 1K–1M; compared to Rac-V12: Rac-V12, *Mad* $p = 0.44$; Rac-V12, *wit* $p = 0.73$). These results suggested to us that BMP signaling may be required for activation of Rac in motor neurons.

BMP Signaling Regulates the Expression of Trio Protein in Motor Neurons

In *Drosophila*, nine of the 22 RhoGEFs identified to date have been shown to be highly expressed in the developing embryonic nervous system (Hu et al., 2005), suggesting possible roles for them in the regulation of nervous system development. Out of these nine GEFs, five have been associated with neuronal growth phenotypes: GEF64C, dPix, ephexin, Still life (Sif), and Trio (Frank et al., 2009; Sanchez-Soriano et al., 2007). We focused on Trio and Sif since they have been shown to act as Rac GEFs and to be expressed in motor neurons (Awasaki et al., 2000; Bateman et al., 2000; Newsome et al., 2000; Sone et al., 1997). In particular, *Drosophila* Trio and its human and *C. elegans* counterparts have been shown to act as Rac GEFs and to participate in the activation of Rac during axon guidance and growth (Awasaki et al., 2000; Bateman et al., 2000; Bateman and Van Vactor, 2001; Briançon-Marjollet et al., 2008; Newsome et al., 2000; Steven et al., 1998). Therefore, we tested the requirement for Trio and Sif for Rac-induced

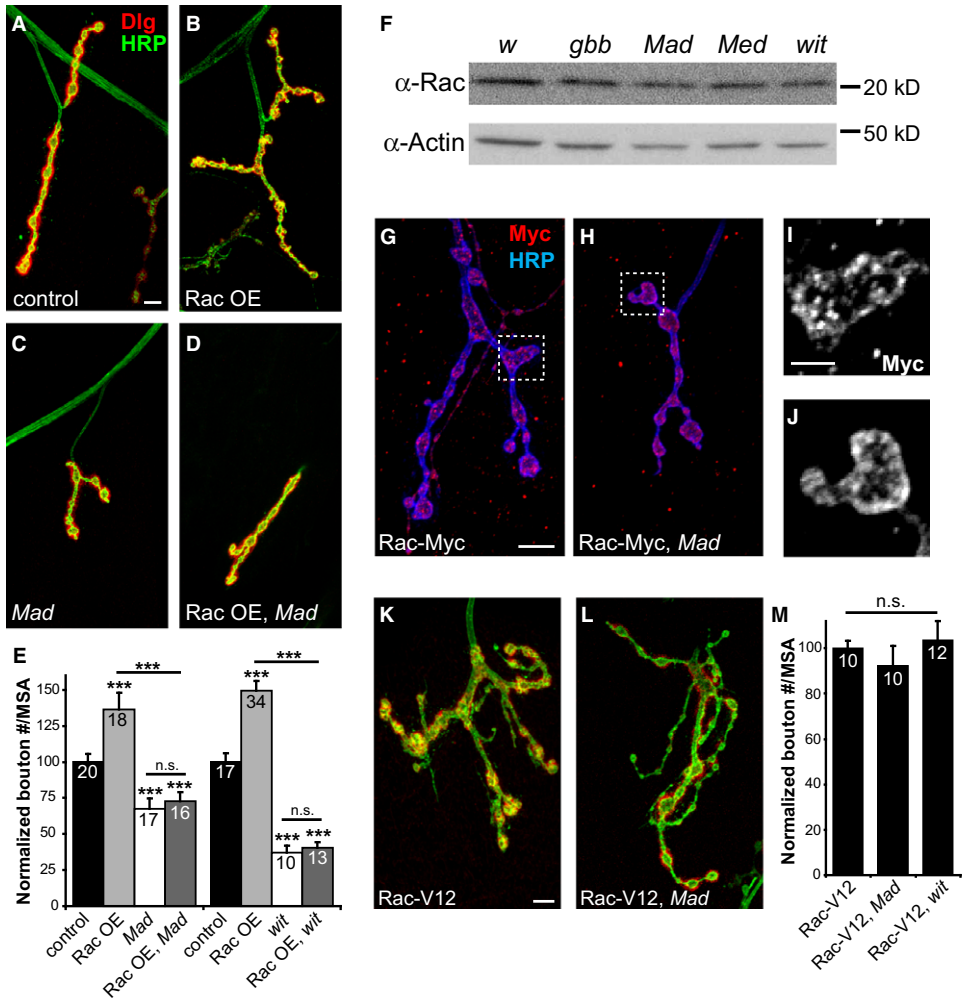

Figure 1. Rac-Induced Synaptic Overgrowth Requires Intact BMP Signaling

(A–D) NMJs stained with anti-Dlg (red) and HRP (green) for (A) control *BG380-Gal4*/+, (B) Rac overexpression *BG380/+; UAS-Rac*/+, (C) Mad^{1}/Mad^{237}, and (D) *BG380/UAS-Rac-Myc;* Mad^{1}/Mad^{237}.

(E) Quantification of bouton number per muscle surface area (MSA) at muscle 4 for the same genotypes as above, as well as for the following *wit* mutants: wit^{A12}/wit^{HA3} and *BG380/+; UAS-Rac/+;* wit^{A12}/wit^{HA3}. *Mad* and *wit* mutants suppress Rac-induced overgrowth.

(F) Western blot for endogenous Rac from larval brain extracts from wild-type (w^{1}), *gbb* (gbb^{2}, *UAS-*Gbb^{99}/gbb^{1}), *Mad* (Mad^{1}/Mad^{237}), *Med* (Med^{G112}/Med^{C246}), and *wit* (wit^{HA2}/wit^{HA3}). The levels of Rac are similar in wild-type and BMP mutant brains.

(G–J) Overexpressed Rac-Myc (red) localizes to the NMJ in both wild-type (G and I, *BG380/UAS-Rac-Myc*) and *Mad* mutant backgrounds (H and J, *BG380/UAS-Rac-Myc;* Mad^{1}/Mad^{237}). (I) and (J) are zoomed in images of the boxed regions from (G) and (H).

(K–L) anti-Dlg (red) and HRP (green) staining of NMJs for (K) constitutively active Rac-V12 overexpression (*BG380/+; UAS-Rac-V12*/+) and (L) Rac-V12 in a *Mad* mutant background (*BG380/+;* Mad^{1}/Mad^{237}*; UAS-Rac-V12*/+).

(M) Quantification of *Mad* and *wit* with Rac-V12 overexpression, normalized to Rac-V12 (same genotypes as above plus *BG380/+; UAS-Rac-V12,* wit^{HA2}/wit^{A12}). The mutants were not able to suppress Rac-V12 overexpansion.

Scale bars: (A, G, and K) 10 μm, (I) 2 μm. Error bars = SEM. See also Figure S1.

NMJ overgrowth by conducting dominant suppression genetic interaction experiments. We found that removal of one copy of the *trio* gene suppressed the Rac-induced increase in synaptic bouton number by more than 50% (percentage of control: Rac OE: 136.03 ± 5.16; Rac OE, *trio*/+: 109.99 ± 4.89, p = 0.006), while loss of one copy of *sif* had no effect (Rac OE, *sif*/+: 125.26 ± 6.23, p = 0.18; Figures 2A–2C).

Based on the findings presented thus far, we hypothesized that BMP signaling may regulate the expression of Trio, thereby influencing Rac activity. To test this hypothesis, we examined Trio protein expression by western blot analysis using head preparations (containing the entire CNS and other tissue) from wild-type larvae and larvae mutant for *gbb*, *Mad*, *Med*, or *Sax*, and for *wit* mutants we compared brain only preparations (Figure 2D). Strikingly, we found a strong reduction in Trio protein in all five mutants (Figures 2D and 2E). Compared to wild-type, *Mad* mutants showed approximately 90% reduction in Trio levels relative to that of actin (p = 0.004). In order to verify the

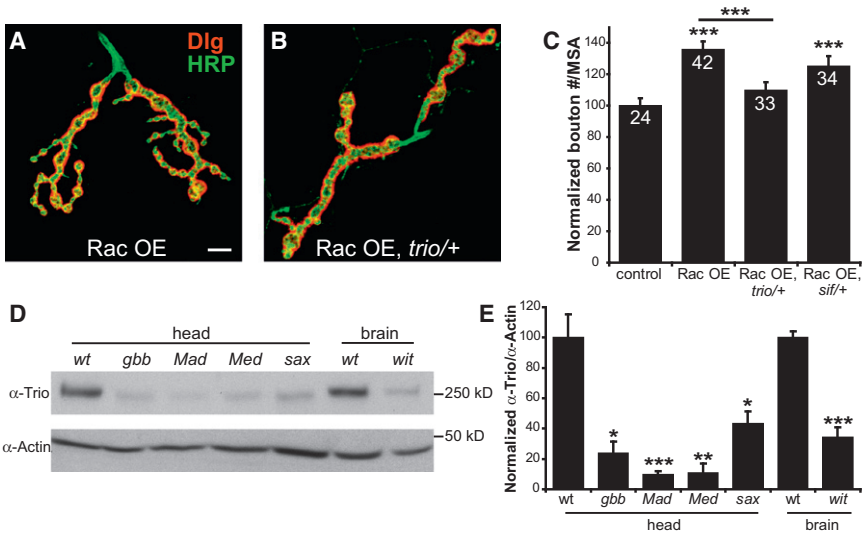

Figure 2. Trio Rac-GEF Levels Are Decreased in BMP Mutants

(A and B) anti-Dlg (red) and HRP (green) NMJ staining for (A) Rac overexpression (*OK6/UAS-Rac*) and (B) *trio* dominant suppression of Rac overexpression (*OK6/UAS-Rac; trio^{S137203}/+*).

(C) *trio* can significantly suppress Rac-induced overgrowth, whereas the GEF *sif* cannot. (*OK6/+* (control); *OK6/UAS-Rac*; *OK6/UAS-Rac; trio^{S137203}/+*; *OK6/UAS-Rac; sif^{ES11}/+*).

(D) Western blot for Trio, using protein extracts from larval heads or brains from the following genotypes: *w^{1}*, *gbb^{2},UAS-Gbb^{99}/gbb^{1}*, *Mad^{1}/Mad^{237}*, *Med^{G112}/Med^{C246}*, and *sax^{4}/sax^{6}* using head extracts, followed by *w^{1}* and *wit^{HA2}/wit^{HA3}* using brains.

(E) Quantification of three western blots for Trio. The intensity of the Trio bands was divided by those for Actin protein to control for potential unequal loading.

Scale bar (A) = 5 μm. Error bars = SEM. See also Figure S2.

specificity of the anti-Trio antibody, which recognizes the C terminus (Awasaki et al., 2000), we also included samples from *trio* mutants and larvae that overexpressed a Trio transgene using BG380-Gal4 (Figure S2).

These results supported our hypothesis and suggested that the BMP signaling cascade at the NMJ normally regulates Trio protein expression, offering an explanation as to why loss of BMP signaling could suppress Rac-induced synaptic growth but failed to affect Rac-V12-induced growth.

Trio Is Required in Motor Neurons for Normal Synaptic Structural Growth at the NMJ

If the regulation of Trio protein levels by BMP signaling were relevant to the control of synaptic growth during larval development, one would expect NMJ growth to be affected in *trio* loss of function mutants. *trio* mutants exhibit strong defects in axon guidance and growth during embryonic development (Awasaki et al., 2000; Bateman et al., 2000; Hakeda-Suzuki et al., 2002; Newsome et al., 2000), but we found that several *trio* mutant combinations could survive until the end of larval stages (Figure 3). We analyzed two of these combinations (*trio^{S137203}* and *trio^{6A}/trio^{S137203}*) by western blot and were unable to detect any Trio protein using an anti-Trio antibody (Figure S2), consistent with previously published reports that designated these as *trio* null alleles (Bateman et al., 2000). In wild-type larvae we occasionally find muscles where an NMJ has not formed; we did not find an increase in the number of muscles without NMJs in *trio* mutants (n = 60). Therefore, it appears that early defects, at least in some *trio* mutant embryos, can be overcome in later stages of development. We examined the number of boutons per MSA in several transallelic *trio* mutant combinations in wandering third instar larvae. Our quantification revealed a significant reduction in the number of synaptic boutons in *trio* larvae, without any effect on muscle surface area (Figures 3B and 3D). The number of boutons per MSA at muscle 4 in *trio* larvae was approximately 35% less than that in control larvae (100 ± 4.41 for control compared to 63.80 ± 5.75 for *trio^{S137203}*, 66.34 ± 4.78 for *trio^{6A}/trio^{S137203}*, and 61.11 ± 4.67 for *trio^{S137203}/Df*, $p < 0.0001$). Based on these results, we conclude that all the *trio* alleles that we used in this study are functionally null. Furthermore, we were able to rescue these defects by providing a UAS-Trio transgene in neurons, but not in muscles (Figures 3A–3D; compared to *trio* mutants, muscle rescue: $p = 0.73$; motor neuron rescue: $p = 0.00041$), suggesting that Trio is required presynaptically for normal synaptic growth at the NMJ. Consistent with our results that *trio* mutants have reduced NMJs, *trio* has been reported to show transheterozygous genetic interaction with the presynaptic receptor phosphatase Dlar at the NMJ, leading to a decrease in bouton number (Pawson et al., 2008).

In order to examine the temporal requirement for Trio during larval NMJ growth, we tested whether presynaptic expression of UAS-Trio during larval stages alone is sufficient to rescue NMJ defects observed in *trio* mutants. Using elav-GS-Gal4, we turned on Trio expression in first instar larvae and kept expressing it until we harvested the wandering third instar larvae for dissection. We found that providing Trio solely during larval stages was sufficient to rescue the synaptic defects in *trio* mutants (Figure 3D).

We further examined the dependence of Rac GTPase function on Trio, by examining the effect of loss of *trio* on Rac or Rac-V12-induced NMJ overgrowth. Loss of *trio* showed strong genetic epistasis with overexpressed Rac (percent of control, Rac OE: 143.14 ± 5.92; Rac OE, *trio*: 66.93 ± 7.47; $p = 0.00060$). On the other hand, genetic removal of *trio* failed to suppress the NMJ overgrowth caused by Rac-V12 overexpression (Figures 3E–3I), further suggesting that Trio is normally required for the activation of Rac in motor neurons.

Finally, we examined the localization of Trio protein at the NMJ using the anti-Trio antibody. We were unable to detect a signal associated with the endogenous Trio; however, we detected a specific accumulation of transgenically expressed Trio in motor neuron terminals using this antibody (Figures 3J–3M). This finding does not conclusively reveal the normal site of action of Trio, but it suggests that Trio can localize to presynaptic sites

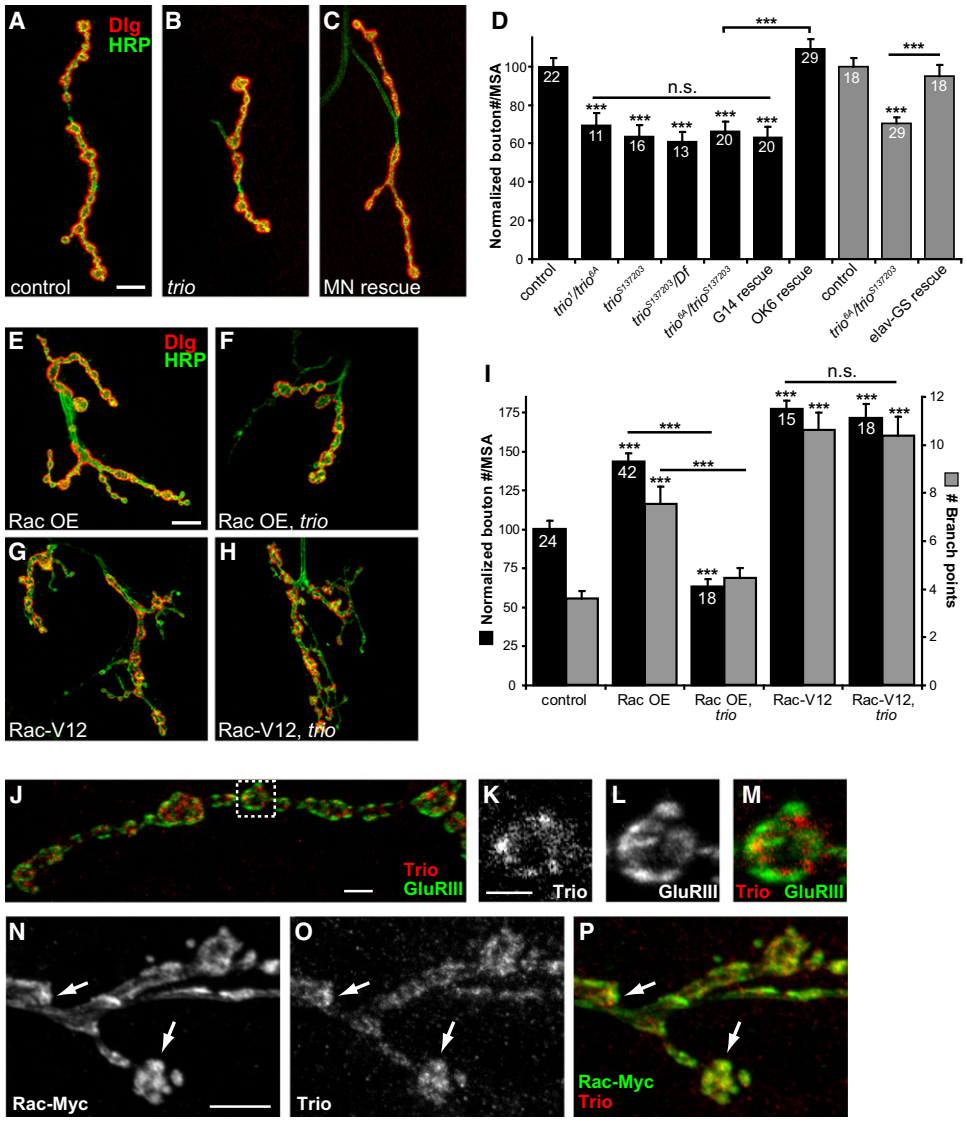

Figure 3. Trio Is Required Presynaptically to Positively Regulate Synaptic Growth

(A–C) Control NMJ (A, $trio^{S137203}$/+), *trio* mutant (B, $trio^{S137203}/trio^{6A}$), and presynaptic rescue of the *trio* mutant (C, *OK6-Gal4/UAS-Trio;* $trio^{S137203}/trio^{6A}$). Anti-Dlg is red and anti-HRP green.

(D) Quantification of NMJ reduction in *trio* mutants and rescue. Loss of *trio* caused an ~35% reduction in bouton number in a variety of genetic backgrounds compared with *OK6*/+ controls. This could not be rescued by expression of the UAS-Trio transgene in muscles (*UAS-Trio*/+; *G14*/+; $trio^{S137203}/trio^{6A}$) but was completely rescued by presynaptic expression using OK6 (*UAS-Trio*/+; *OK6*/+; $trio^{S137203}/trio^{6A}$). *trio* could also be rescued by expressing UAS-Trio in the nervous system only in larval stages using elav-GeneSwitch-Gal4 (gray bars; control: *UAS-Trio*/+; $trio^{6A}$/+. elav-GS rescue: *UAS-Trio*/+; *elav-GS*/+; $trio^{S137203}/trio^{6A}$).

(E–H) Representative NMJs stained with Dlg (red) and HRP (green) for (E) Rac overexpression (*OK6*/*UAS-Rac*), (F) suppression of Rac overgrowth by *trio* (*OK6*/*UAS-Rac;* $trio^{S137203}$/ $trio^{S137203}$), (G) Rac-V12 overexpression (*BG380*/+;*UAS-Rac-V12*/+), and (H) loss of *trio* in the Rac-V12 background (*BG380*/+; $trio^{S137203}$/ *UAS-Rac-V12,* $trio^{6A}$), which does not suppress the Rac-V12 overgrowth, similar to BMP mutants.

(I) Quantification for genotypes in (E)–(H) for both bouton number (black bars) and for number of branch points (gray bars).

(J–M) anti-Trio (red) and anti-GluRIII (green) staining of an NMJ overexpressing Trio (*BG380*/*UAS-Trio*). (K–M) are zoomed in images of the boxed bouton in (J), showing the close apposition between Trio staining and postsynaptic GluR puncta.

(N–P) Boutons from an NMJ overexpressing both UAS-Trio and UAS-Rac-Myc (*BG380*/*UAS-Rac-Myc; UAS-Trio*/+), stained for anti-Myc (N) and anti-Trio (O). Arrows point to two puncta that show colocalization in (P).

Scale bars: (A and E) 10 μm, (J) 2 μm, (K) 1 μm, (N) 5 μm. Error bars = SEM. See also Figure S3.

and in some cases in close apposition to postsynaptic densities (Figure 3M). Also, we found that the distribution of Trio overlapped with that of Rac-Myc when both these transgenes were coexpressed in motor neurons (Figures 3N–3P). In order to explore the site of action of Rac further, we generated a GFP Rac transgene carrying the entire 5′ and 3′ UTR of Rac

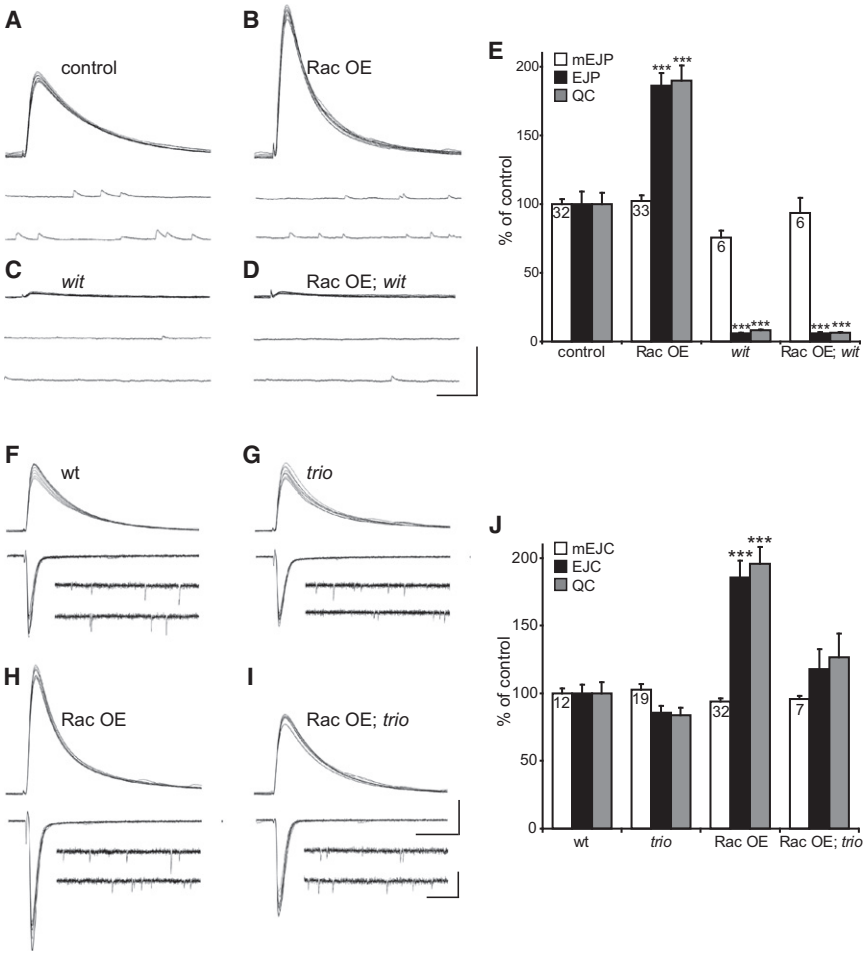

Figure 4. Synaptic Release Is Increased in Rac Overexpression and Suppressed by *wit* and *trio* Mutants

(A–D) Example current clamp recordings of evoked response (top) and miniature EJPs (bottom) for control (A, *BG380/+*), Rac overexpression (B, *BG380/+; UAS-Rac/+*), *wit* mutant (C, wit^{A12}/wit^{HA2}), and Rac overexpression in *wit* mutants (D, *BG380/+; UAS-Rac/+;* wit^{A12}/wit^{HA2}). Scale bar for EJP: 10 mV/40 ms and mEJP: 10 mV/400 ms.

(E) Quantification of mEJP amplitude, EJP amplitude and quantal content for the genotypes in (A)–(D) normalized to control.

(F–I) Sample EJP recordings (top), voltage-clamped EJCs (bottom) and mEJCs (bottom inset) for wild-type (F, w^1/w^{1118}), *trio* mutant (G, $trio^{6A}/trio^{S137203}$), Rac overexpression (H, *OK6/UAS-Rac*), and mutant *trio* in Rac overexpression (I, *OK6/UAS-Rac;* $trio^{S137203}/trio^{S137203}$). EJC: 10 nA/40 ms; mEJC: 2 nA/400 ms.

(J) Quantification of voltage clamp data for the same genotypes in (F)–(I). Loss of *trio* suppresses the increase in quantal content caused by Rac overexpression.

Error bars = SEM.

(UAS-GFP-Rac), with the hope that this transgene would closely mimic the endogenous expression of Rac. Similar to the Rac-Myc transgene, we found that GFP-Rac accumulated in axons and at the NMJ but avoided any nuclear localization (Figure S3). This finding suggests that Rac-induced synaptic overgrowth does not involve nuclear signaling, in contrast to Rac's function in epithelial planar polarity (Fanto et al., 2000).

Together, these results highlight the requirement for Trio in motor neurons for normal synaptic growth and by extension the importance of Rac GTPase activity during intense synaptic growth in larvae.

Rac-Induced NMJ Growth Is Accompanied by an Increase in Neurotransmitter Release

The strong induction of synaptic structural growth by Rac overexpression prompted us to ask whether Rac overexpression in motor neurons can also enhance synaptic strength. Pharmacological manipulations of actin dynamics have been shown to influence synaptic release in cultured primary neurons as well as at the larval NMJ (Kuromi and Kidokoro, 2005; Morales et al., 2000). Using intracellular recordings in wandering third-instar larvae, we found that indeed overexpression of Rac can lead to a significant increase in the amount of neurotransmitter release (Figures 4A and 4B). While the size of miniature excitatory junctional potentials (mEJPs) was not statistically different from that of controls, the mean size of the evoked excitatory junctional potentials (EJPs) was greatly increased in response to Rac overexpression, indicating a significant increase in quantal content (QC) (Figures 4A, 4B, and 4E). Consistent with our previous results, we found that the increase in QC was dependent on normal BMP signaling in motor neurons, as loss of *wit* fully suppressed the Rac-induced increase in neurotransmitter release (Figures 4C–4E).

We then wished to evaluate the role of Trio in the regulation of synaptic release at the NMJ. For these experiments, we used a standard two-electrode voltage clamp technique to record excitatory junctional currents (EJCs) and miniature EJCs (mEJCs) in wandering third-instar larvae. We found a downward trend in average EJC size and quantal content in *trio* mutant larvae compared to wild-type larvae (Figures 4F, 4G, and 4J; QC: 25.59 ± 2.12 for wild-type compared to 21.45 ± 1.37 for *trio* mutants); however, the differences were not statistically significant ($p = 0.096$ by t test). While basal electrophysiological properties appeared unaffected in *trio* mutants, we found that Trio is essential for the Rac-induced enhancement in quantal release. Genetic removal of *trio* restored normal synaptic function in larvae overexpressing Rac in motor neurons (Figures 4H–4J). These results further establish a link between Rac-GTPase activity and synaptic growth at the NMJ and at the same time suggest that structural modifications and changes in neurotransmitter release have differential sensitivities to the levels of Rac-GTPase activity in motor neurons.

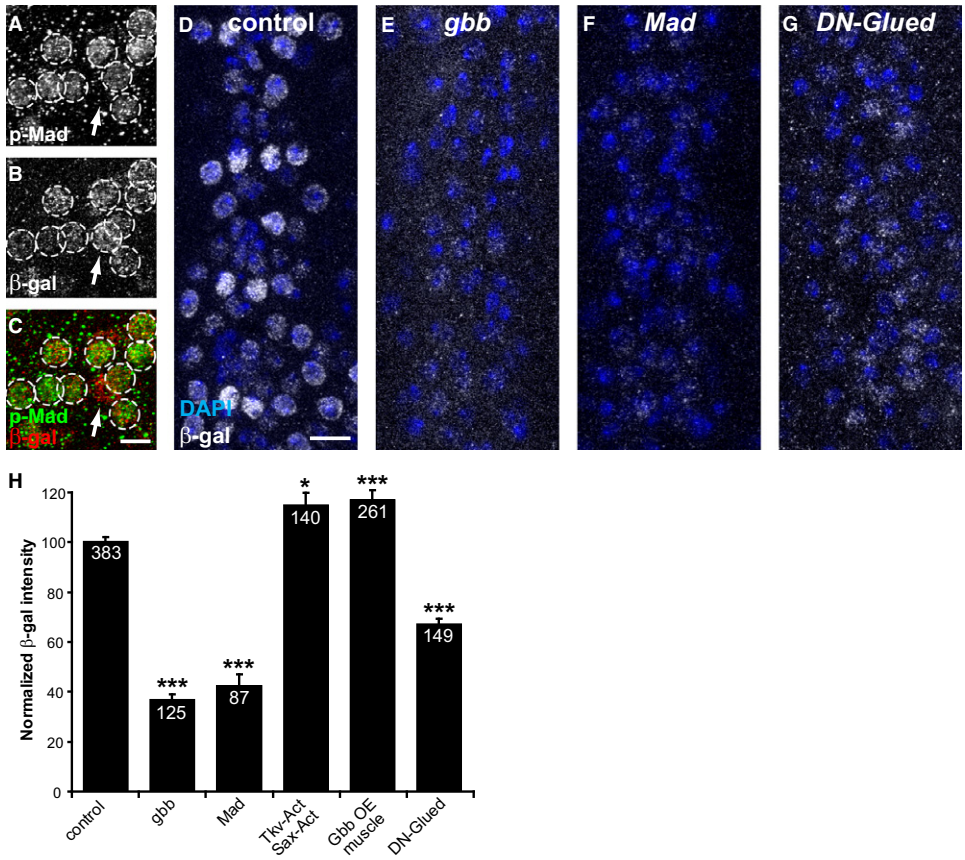

Figure 5. *trio* Transcriptional Activity in Motor Neurons Is Regulated by Retrograde BMP Signaling

(A–C) The LacZ enhancer trap reporter in the first exon of the *trio* gene shows expression in motor neurons (β-gal staining in red) in the larval ventral nerve cord in the same cells expressing p-Mad (green). Motor neurons that show co-staining for p-Mad and β-gal are circled and one cell body that shows β-gal signal but no detectable p-Mad signal is pointed out with the arrow.

(D–G) Confocal projections of motor neurons in VNCs stained for β-gal (white) and DAPI (blue) in control ($trio^{S137203}$/+), *gbb* mutants (gbb^{2}, $UAS\text{-}Gbb^{99}/gbb^{1}$; $trio^{S137203}$/+), *Mad* mutants (Mad^{1}/Mad^{12}; $trio^{S137203}$/+) and presynaptic expression of DN-Glued (*BG380/+; UAS-DN-Glued*^{84,96B}/+ $trio^{S137203}$/+).

(H) Quantification of average β-gal intensity in motor neurons in the above genotypes as well as in larvae overexpressing activated Tkv and Sax (*UAS-TkvA,SaxA/+; OK6/+;* $trio^{S137203}$/+) in motor neurons or overexpressing Gbb in the muscle (*G14/UAS-Gbb*^{94}*;* $trio^{S137203}$/+).

Error bars = SEM. See also Figure S4.

trio Transcriptional Activity in Motor Neurons Requires Retrograde BMP Signaling

The effect of loss of BMP signaling on Trio protein expression raises the possibility that *trio* transcription may be regulated by BMP signaling in motor neurons. To test if *trio* transcription is affected in motor neurons, we took advantage of $trio^{S137203}$ flies that contain a LacZ reporter in the first exon of the *trio* gene (abbreviated *trio* LacZ; Bateman et al., 2000). Based on its location within the gene, levels and patterns of LacZ expression in these animals would be expected to reflect *trio* transcription closely. Using an anti-β-D-galactosidase (β-gal) antibody, we could detect β-gal signal in a large population of neurons including motor neurons in the medial section of the third instar ventral nerve cord (VNC) in heterozygous $trio^{S137203}$ larvae (Figures 5A–5D). We and others have used the presence of phosphorylated Mad (p-Mad) in these neurons as an indication of active BMP signaling (Marqués et al., 2002; McCabe et al., 2003; Merino et al., 2009). We found that the β-gal signal associated with *trio* LacZ insert showed nearly complete overlap with the p-Mad signal (Figures 5A–5C). In rare cases, the p-Mad signal was below detection level in β-gal-positive nuclei (arrow in Figure 5A). We then tested the effect of loss or gain of BMP signaling on LacZ expression in heterozygous $trio^{S137203}$ larvae. Loss of *Mad* or *gbb* caused a drastic decrease in β-gal signal (Figures 5D–5F and 5H; control: 100 ± 1.92, *gbb*: 36.78 ± 1.92, *Mad*: 42.28 ± 4.36, $p < 0.0001$), while overexpression of constitutively active forms of BMP type I receptors Thick veins (Tkv) and Sax led to an enhancement of the signal (Figure 5H; 114.89 ± 4.94, $p = 0.011$). We then tested whether BMP signaling can modulate transcriptional activity of *trio* via retrograde signaling from muscles to motor neurons. For this, we first measured the level of β-gal signal in *trio* LacZ heterozygous larvae in response to overexpression of a Gbb transgene in all muscles using G14-Gal4 (Aberle et al., 2002) and found a significant increase in the level of β-gal signal (Figure 5H; 116.95 ± 3.74, $p < 0.0001$). Second, we tested the consequence of

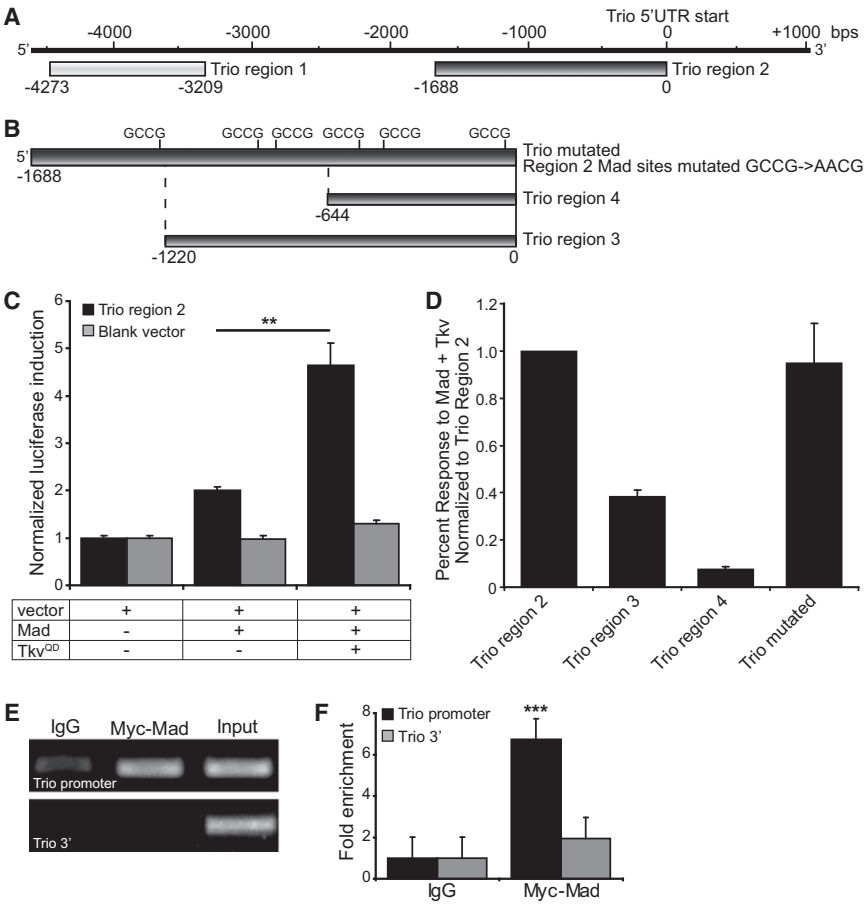

Figure 6. Mad Directly Binds the *trio* Promoter

(A) Genomic region upstream of *trio* open reading frame. Shaded boxes indicate regions 1 and 2 tested with the luciferase reporter assay. Trio region 1 showed no luciferase induction and was not tested further.

(B) Illustration of Trio region 2 deletions of 1044 bps (Trio region 4) and 468 bps (Trio region 3), and Mad consensus sites mutated from GCCG to AACG (Trio mutated).

(C) In vitro luciferase assay in HEK293 cells expressing a combination of a luciferase reporter vector (with or without Trio region 2 upstream of luciferase), Mad, and activated Tkv (Tkv^{QD}). Coexpressing Tkv^{QD} with Mad significantly increases luciferase induction in the presence of the *trio* promoter (n = 6). A blank vector, without the *trio* promoter, showed no change in luciferase expression in response to Mad/Tkv^{QD} (n = 3).

(D) Luciferase induction by Mad/Tkv^{QD} with the Trio regions illustrated in (A) and (B). Responses are expressed as a percentage normalized to the average Trio region 2 response to Mad/Tkv^{QD}.

(E and F) A ChIP assay was performed on embryos expressing Myc-Mad in motor neurons (*BG380, UAS-Myc-Mad/+*), using Myc antibodies or IgG as a negative control. Conventional PCR (E) and real-time PCR (F; n = 3) reveal that Myc-Mad associates with the putative *trio* promoter region, upstream of the transcriptional start site, but not with a downstream region of the *trio* gene, near the 3′ end of the coding region (Trio 3′).

Error bars = SEM.

disruption of retrograde axonal transport on transcriptional activity of *trio*. For this, we overexpressed a dominant negative Glued transgene in all motor neurons. Glued is the *Drosophila* homolog of vertebrate Dynactin, the cytoplasmic Dynein activating protein, and its dominant-negative form has been used to disrupt retrograde axonal transport and BMP signaling (McCabe et al., 2003). Disruption of retrograde axonal transport led to a significant reduction in β-gal signal in motor neurons (Figures 5G and 5H; 67.14 ± 2.10, $p < 0.0001$).

Finally, we analyzed the levels of *trio* transcript in the embryonic and larval nervous system by conducting in situ hybridization experiments. Previously, it has been demonstrated that *trio* transcript is highly enriched in late embryonic central and peripheral nervous system (Bateman et al., 2000). Our experiments support this finding (Figure S4) and extend these results to show that loss of BMP signaling in *Mad* mutants significantly reduces the level of *trio* mRNA expression in the embryonic nervous system and larval ventral nerve cord (Figure S4).

Mad Directly Interacts with the *trio* Promoter

While these findings provide strong evidence for the regulation of transcriptional activity at the *trio* locus via retrograde BMP signaling, they fall short of indicating whether *trio* is a direct transcriptional target of BMP signaling. To address this, we conducted two sets of experiments. First, we tested whether the predicted *trio* promoter would respond to activation of Mad in an in vitro promoter reporter assay. We focused on two regions within the putative *trio* promoter based on the presence of high numbers of minimal Mad consensus (GCCG) sequences (Figure 6A; Kusanagi et al., 2000). In transfected HEK293 cells, we found that baseline luciferase activity under the control of region 2 showed an approximately 5-fold increase in response to overexpression of Mad and constitutively active Tkv receptor (Figure 6C); in contrast, region 1 did not respond to Mad/Tkv activation (data not shown). Next, we truncated Trio region 2 into smaller regions (Figure 6B) and found that the removal of the first ~450 bases significantly reduced the ability of region 2 to respond to Mad/Tkv. Further truncation of the promoter suggested that the first 1000 bases are necessary for efficient Mad interaction with the promoter as the removal of this region completely abolished the transcriptional response to Mad/Tkv (Figure 6D). Finally, to test the potential role of GCCG sites, we mutated all six sites in region 2 to AACG; however, this had little effect on the ability of the promoter to respond to Mad/Tkv (Figure 6D). These findings identify a region in the *trio* promoter that is responsible for conferring Mad/Tkv sensitivity and at the same time suggest that Mad interaction with the promoter cannot be predicted simply based on short consensus sequences.

Second, we conducted chromatin immunoprecipitation (ChIP) assays to examine the association of Mad with he

endogenous promoter/enhancer of *trio* in motor neurons. For these experiments, we overexpressed a Myc-tagged Mad transgene in all motor neurons using BG380-Gal4 and performed immunoprecipitation using an anti-Myc antibody in late embryonic preparations. We then conducted PCR using the immunoprecipitated DNA with two sets of primers: one against the predicted promoter region and one against the 3′ end of *trio*, approximately 1 kb upstream from the end of the coding region (Figure 6E). We found a prominent product of the predicted size using the promoter primer set but no band using the 3′ coding primer set, while both products were detected from preparations prior to immunoprecipitation (designated Input; Figure 6E). We verified these results using quantitative PCR and found a 6-fold enrichment in *trio* promoter DNA associated with Myc-Mad than associated with the negative control IgG (Figure 6F). These findings together provide strong evidence that normally BMP signaling directly regulates transcription from the *trio* locus.

Providing Trio in Motor Neurons Can Partially Rescue NMJ Defects in BMP Mutants

Based on our findings thus far, one would predict that the observed decrease in *trio* expression in motor neurons in *Mad* or *wit* mutants may be at least partially responsible for the NMJ growth defects in these mutants. If this prediction is true, then we would expect double mutants of *trio* and *Mad* to look no worse than *Mad* single mutants. Indeed, we find no difference in bouton number between *Mad* mutants and *Mad; trio* double mutants (Figures 7A–7C and 7G; percent of control, *Mad*: 53.81 ± 6.55, *Mad; trio*: 60.96 ± 3.22, p = 0.33). Based on the same logic, one would expect that providing Trio in motor neurons should at least partially rescue synaptic defects associated with reduced BMP signaling in motor neurons. We tested this possibility by overexpressing a Trio transgene in *Mad* or *wit* mutant larvae. Consistent with our prediction, we found that motor neuronal overexpression of a Trio transgene in *Mad* and *wit* mutant larvae led to a significant enhancement of the number of synaptic boutons per MSA (Figure 7; control: 100 ± 5.22, *Mad*: 62.46 ± 4.79, *Mad*, Trio OE: 81.94 ± 4.22, p = 0.0047 with *Mad*; *wit*: 33.28 ± 3.87, *wit*, Trio OE: 56.01 ± 4.36, p = 0.0019 with *wit*). Overexpression of the same transgene in wild-type larvae did not lead to any change in NMJ growth (Figure 7G, *BG380/UAS-Trio*: 95.14 ± 7.91, p = 0.32).

We did not find a significant rescue of the electrophysiological defects in *wit* mutants in a similar experimental setting (data not shown), consistent with our previous results that growth of synaptic structures and regulation of neurotransmitter release have different sensitivities to BMP signaling and the level of Rac-GTPase activity (Figure 4; Goold and Davis, 2007; Merino et al., 2009). We further explored the interaction between *trio* and BMP signaling in the regulation of synaptic release. Increased BMP signaling in motor neurons leads to an increase in synaptic release at the NMJ (Rawson et al., 2003) without affecting the number of synaptic boutons (McCabe et al., 2004; Merino et al., 2009). Based on our results thus far, one would predict that removal of Trio would counteract the effect of increased BMP signaling in motor neurons. We tested this by comparing wild-type and *trio* mutant larvae expressing activated Tkv and

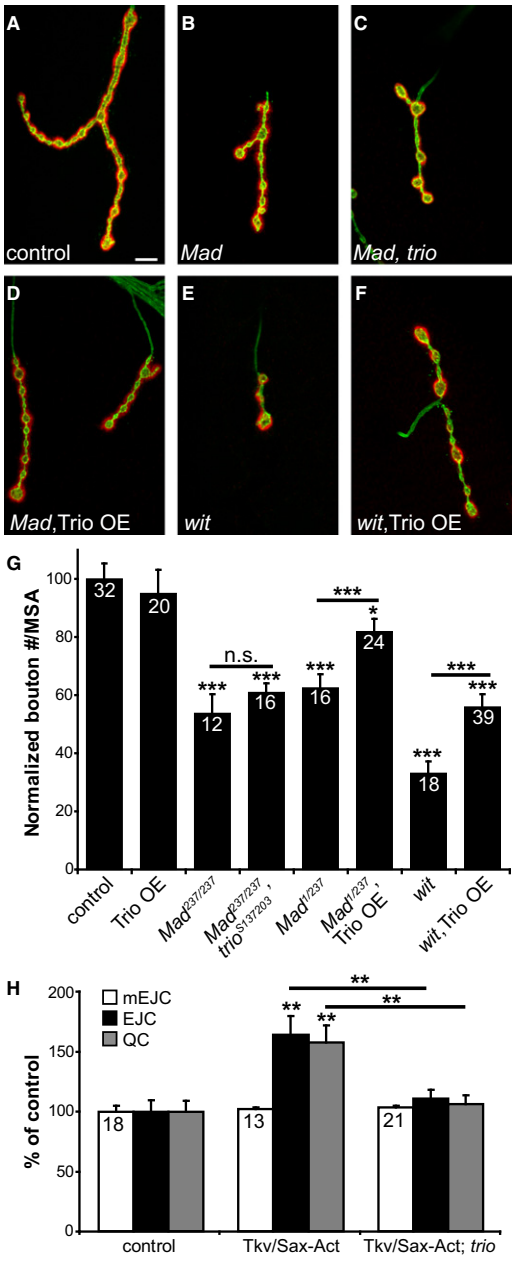

Figure 7. Presynaptic Trio Expression Can Partially Rescue *Mad* and *wit* Mutants

(A–F) Representative NMJs stained with anti-Dlg (red) and HRP (green) for (A) control (*BG380/+;Mad*^{1}*/+*), (B) *Mad* mutant (*UAS-Trio/+;Mad*^{1}*/Mad*^{237}), (C) *Mad, trio* double mutants (*Mad*^{237}*/Mad*^{237}, *trio*^{S137203}*/ trio*^{S137203}), (D) *Mad* rescued by overexpression of Trio (*BG380/UAS-Trio; Mad*^{1}*/Mad*^{237}), (E) *wit* mutant (*BG380/+; wit*^{A12}*/wit*^{HA2}), and (F) *wit* rescued by Trio overexpression (*BG380/UAS-Trio; wit*^{A12}*/wit*^{HA2}).

(G) Quantification of number of boutons per MSA for above genotypes as well as for Trio overexpression (*BG380/UAS-Trio*).

(H) Quantification of mEJC, EJC, and quantal content normalized to the control (*BG380/+*) for activated Tkv and Sax (*BG380/UAS-TkvA,SaxA*), and for suppression of activated Tkv/Sax by *trio* (*BG380/UAS-TkvA,SaxA; trio*^{6A}*/ trio*^{S137203}).

Scale bar (A) 5 μm. Error bars = SEM.

Sax receptors in motor neurons. We found that loss of *trio* fully suppressed the increase in EJC and quantal content (Figure 7H). These results together provide a strong functional link between BMP signaling and Trio in promoting synaptic growth and function at the NMJ.

DISCUSSION

Our findings provide genetic and biochemical evidence for a model in which the retrograde BMP signaling cascade at the larval NMJ orchestrates the growth of synaptic boutons in part by controlling the expression of the Rac GEF Trio in motor neurons. We show that both Trio protein and *trio* transcriptional activity in motor neurons are dependent on retrograde Gbb signaling from postsynaptic muscles, as well as on the presence of BMP receptors and transcription factors in presynaptic motor neurons. Reminiscent of loss of BMP signaling, *trio* loss of function leads to severe structural defects at the NMJ. We demonstrate that transgenic expression of Trio in *Mad* and *wit* mutant larvae can significantly restore NMJ structures in these mutants. These findings together provide strong evidence that Trio acts downstream of retrograde BMP signaling in motor neurons to regulate the robust synaptic growth that occurs during larval development.

How Does Trio Control Synaptic Growth in Response to BMP Signaling?

The instructive role of small GTPases in inducing changes in axon growth and guidance is well established and several signal transduction pathways have been shown to link guidance receptors to the actin cytoskeleton via their regulation of Rho family GTPase activity in these processes (Dickson, 2001; Fan et al., 2003; Luo, 2000; Pawson et al., 2008). Similarly, in vertebrate neuronal cultures and slice preparations, the vertebrate homolog of Trio and other GEFs such as Kalirin and Intersectin have been shown to act on small GTPases to influence axon guidance and growth as well as spine formation (Briançon-Marjollet et al., 2008; Ma et al., 2003; Thomas et al., 2009). At the larval NMJ, we find that Rac-induced synaptic growth is dependent on Trio which is itself under the control of BMP signaling. Importantly, reduced synaptic growth in both *trio* and *Mad* mutants can be fully rescued by overexpression of a GEF-independent form of Rac, Rac-V12. In support of a role for Rac GTPase function in regulating synaptic growth at the NMJ, we find that partial loss of all three Rac genes led to a mild but statistically significant reduction in the number of boutons per MSA at the NMJ (*Rac1*−/+, *Rac2*−/+, *Mtl*−/−: 87.99 ± 2.98 percent of wild-type, p = 0.020; Figure S1F). We were unable to examine the consequence of complete loss of Rac genes, as such genetic combination causes early embryonic lethality (Hakeda-Suzuki et al., 2002).

Based on our findings, we propose that the action of retrograde BMP signaling via Trio leads to the modulation of Rac GTPase activity in motorneurons (Figure 8). While we cannot at this time conclusively demonstrate the subcellular localization of endogenous Rac, our transgenic experiments suggest that it can localize to synaptic structures while avoiding the nucleus. Therefore, we propose that once activated by Trio, whether locally at the synapse or at an upstream site in the axon or cell body, Rac will exert its action primarily locally at the NMJ (Figure 8).

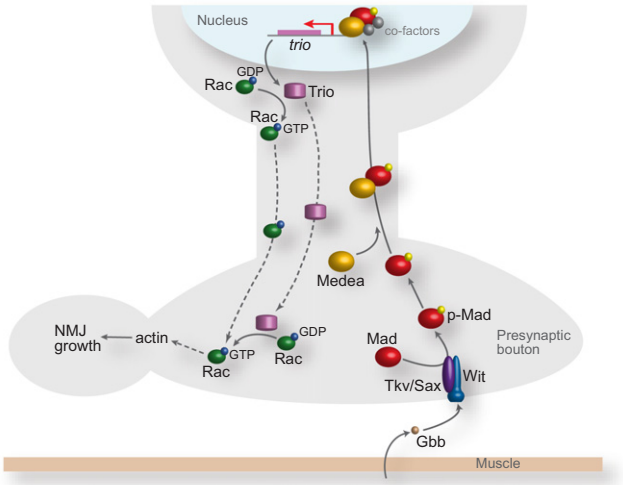

Figure 8. Model of BMP Regulation of *trio* Transcription and Subsequent Rac GTPase Activation

The cartoon proposes a model in which the BMP ligand Gbb, released from the muscle, interacts with a BMP type I/type II receptor complex including Sax/Tkv and Wit at the presynaptic motor neuron terminals leading to phosphorylation of Mad. Phosphorylated Mad translocates from the NMJ to the nucleus upon coassembly with the co-Smad Medea. Mad directly binds the *trio* promoter presumably with cofactors and enchances transcription of *trio*. Trio then activates Rac either in the cell body or at the synapse, which leads to changes in actin cytoskeleton and modulation of synaptic growth.

How Does GTPase Activity Lead to Cytoskeletal Rearrangements at the Synapse?

A number of molecules have been found to act as effectors downstream of Rho GTPases; kinases, in particular, form an important class of Rho family GTPase effectors (Bishop and Hall, 2000). One attractive candidate to act downstream from Rac in motor neurons is the p21 activated kinase (Pak) (Fan et al., 2003; Ng and Luo, 2004; O'Donnell et al., 2009). However, loss of *pak* had no significant effect on Rac-induced synaptic growth at the NMJ (percent of control bouton #/MSA, Rac OE: 136.00 ± 10.59, Rac OE; pak^{6}/+: 115.27 ± 9.12, n = 12, p = 0.15). Also, we found that overexpression of a mutant Rac transgene (Rac-Y40C) that is defective for its ability to interact with Pak (Joneson et al., 1996; Ng et al., 2002) was capable of inducing synaptic overgrowth at the NMJ similarly to a wild-type Rac transgene (Figure S1G). In addition, while Pak is present in motor neurons, it is not detectable in presynaptic terminals (Albin and Davis, 2004; Parnas et al., 2001). Therefore, Pak is not likely to act downstream of Trio and Rac in inducing presynaptic growth. Another attractive candidate for mediating Rac-GTPase action at the NMJ is the Wave/Scar complex. Several members of this complex, including CYFIP, Kette, Scar, and HSPC300 have been implicated in the regulation of NMJ structural growth (Qurashi et al., 2007; Schenck et al., 2004). Interestingly, Rac has been shown to signal through the Wave/Scar complex to induce actin nucleation and lamellipodia formation via the Arp2/3 complex (Eden et al., 2002; Innocenti

et al., 2004). Consistently, we find that a mutant Rac transgene (Rac-F37A) (Ng et al., 2002) that is thought to be defective for its role in inducing lamellipodia formation does not induce synaptic growth as efficiently as a wild-type Rac transgene (Figure S1G). Therefore, it is conceivable that aspects of Rac-induced synaptic growth may be relayed through members of the Wave/Scar family.

GEFs as Transducers of Extracellular Cues at the Synapse

A large body of evidence suggests that regulation of Rho family GTPases in neurons is achieved in large part via regulation of the activity of GEFs and GAPs (O'Donnell et al., 2009). The role of GEFs in linking cell surface cues to cytoskeletal rearrangement is particularly well described during axon growth and guidance (Hu et al., 2005; O'Donnell et al., 2009; Shamah et al., 2001). Similarly, GEFs have been shown to participate in transducing cues from the cell surface to Rho GTPases at the synapse leading to changes in spine formation and dynamics (Lai and Ip, 2009). For example, activation of the EphB receptor induces phosphorylation of two Rac-GEFs, Kalirin and Tiam1, leading to activation of Rac and thereby an increase in spine formation in cultured hippocampal neurons (Penzes et al., 2001; Tolias et al., 2007). It appears that posttranslational modification, interaction with second messengers, as well as protein-protein interaction are some of the main mechanisms through which GEFs are regulated in neurons and other cells (Bos et al., 2007; Penzes et al., 2001). Our findings further our understanding of how growth-promoting cues are linked through the action of GEFs to the cytoskeleton in presynaptic terminals and provide new insights into the regulation of GEFs by demonstrating that transcriptional regulation can play an important role especially during development.

EXPERIMENTAL PROCEDURES

Fly Genetics

Flies were raised on standard medium at 25°C. For Gene Switch experiments, flies were grown on semi-defined medium for 2 days and first-instar larvae were then transferred to food with 200 μM RU486 (Sigma). Fly strains used in this study include: UAS-Rac1, UAS-Rac1-V12 (Luo et al., 1994), and UAS-Rac1-Myc (Ng et al., 2002); UAS-Myc-Rac1-F37A and UAS-Myc-Rac1-Y40C (Ng et al., 2002); UAS-Rho1-V14 (Strutt et al., 1997) and Ub-Cdc42 (Rodal et al., 2008); $Rac1^{J11}$, $Rac2^{\Delta}$ (Ng et al., 2002), Mtl^{Δ} (Hakeda-Suzuki et al., 2002), and Df(3R)BSC497; UAS-Myc-Mad (Merino et al., 2009); Mad^{1}, Mad^{k00237} (abbreviated Mad^{237}) and Mad^{12} (Galindo et al., 2002; Sekelsky et al., 1995); wit^{A12}, wit^{HA2} and wit^{HA3} (Aberle et al., 2002; Marqués et al., 2002); gbb^{1}, gbb^{2}, UAS-Gbb^{99}, and UAS-Gbb^{94} (McCabe et al., 2003; Wharton et al., 1999); Med^{G112} and Med^{C246} (McCabe et al., 2004); sax^{4}, sax^{6}, UAS-SaxA, and UAS-$TkvA^{BX}$ (Hoodless et al., 1996; McCabe et al., 2004; Twombly et al., 1996, 2009); UAS-DN-$Glued^{84,96B}$ (McCabe et al., 2003); UAS-Trio, $trio^{1}$, $trio^{S137203}$, $trio^{6A}$, and Df(3L)Ar12-1 (Bateman et al., 2000; Newsome et al., 2000); sif^{ES11} (Sone et al., 2000); the neuronal drivers OK6-Gal4 (Aberle et al., 2002), BG380-Gal4 (Budnik et al., 1996), elav-GeneSwitch-Gal4 (abbreviated elav-GS) (Osterwalder et al., 2001), $elav^{C155}$-Gal4 (Lin and Goodman, 1994); the muscle drivers MHC-Gal4 (Schuster et al., 1996) and G14-Gal4 (Aberle et al., 2002). Wild-type stocks used were w^{1}, w^{1118}, and *yw*.

Luciferase Assay

HEK293 cells were transfected with psiCheck-2 or regions of *trio* (see Supplemental Information), with and without pcDNA3-Myc-Mad and pcDNA3-HA-Tkv^{QD} (from Esther Verheyen) (Inoue et al., 1998; Zeng et al., 2007) with Lipofectamine 2000 (Invitrogen). After 48 hr, cells were harvested and the luciferase activity was measured with the Dual Luciferase Reporter Assay System (Promega) on a Lumat Single Tube Luminometer LB 9507 (Berthold Technologies). *Renilla* luciferase activity was normalized to firefly luciferase for each transfection to control for transfection and expression levels.

Chromatin Immunoprecipitation

Embryos expressing Myc-Mad in motor neurons were collected for 16 hr and dechorionated in bleach for 3 min. Embryos were fixed in 0.5% formaldehyde for 15 min as previously described (Birch-Machin et al., 2005). After nuclei were isolated and the chromatin was sonicated, part of the DNA was removed for input control, and the rest was incubated with either normal mouse IgG (4 μg, SC-2025 [Santa Cruz Biotechnology]) or mouse anti-Myc (4 μg, 9E10 [DSHB]). Traditional PCR and qPCR (with iQ SYBR Green mix [BioRad]) were performed using primers for the *trio* promoter region: 5′- TGCAGGA GGTAATGCGGCGT and 5′-GCTGAGGGCCAACGATGCCA and using control primers for the 3′ end of the *trio* coding region: 5′-TGAGGACCTGAAGG GTGGTA and 5′- ATGTATTCGGACAGCGGTTT.

Western Blots

Protein was extracted from heads or brains from third instar larvae as previously described (Merino et al., 2009). The following antibodies were used: anti-Rac (clone 102, 1:500, Millipore), anti-Trio (9.4A, 1:250, DSHB), and anti-Actin (1:2000, Millipore). The proteins were visualized using HRP-conjugated secondaries (1:5000, Molecular Probes).

Electrophysiology

Intracellular recordings were performed on muscle 6, segment A3 in dissected third-instar larvae (Haghighi et al., 2003). Larvae were prepared for recording in physiological saline HL3 (Stewart et al., 1994) containing 0.5 mM Ca^{2+}. mEJPs and EJPs were recorded first and then the muscle was voltage clamped (using two-electrode voltage clamp technique) to measure currents. Muscles with initial membrane potential less than −65 mV and input resistance less than 5MΩ were rejected. For voltage clamp experiments the amount of current needed to inject to clamp the muscle at −80mV was less than 4nA. Details of data analysis are provided in Supplemental Experimental Procedures.

Immunohistochemistry

Third-instar larvae were dissected in HL3 and fixed in 4% paraformaldehyde for 10 min as previously described (Stewart et al., 1994). The following primary mouse antibodies were obtained from the Developmental Studies Hybridoma Bank (DSHB): anti-Discs Large (4F3, 1:250), anti-Myc (9E10, 1:500), anti-Trio (9.4A, 1:250), and anti-β-gal (40-1A, 1:100). In addition, we used rabbit anti-Myc (1:100, Cell Signaling), rabbit anti-GFP (1:500, Molecular Probes), rabbit anti-DGluRIII (1:2500, gift from A. DiAntonio), rabbit anti-p-Mad (PS1, 1:100, provided by P. ten Dijke), and Cy5-conjugated goat anti-HRP (1:125; Jackson ImmunoResearch Laboratories). Secondary antibodies were Alexa-488-conjugated goat anti-rabbit and anti-mouse (1:500, Molecular Probes) and Cy3-conjugated goat anti-rabbit and anti-mouse (1:500, Amersham Bioscience). DAPI was used at 1:10,000 (Sigma-Aldrich).

Imaging and Data Analysis

Muscle 4 from segment 3 was analyzed, unless otherwise stated. Bouton counts and other structural analyses were done under 63× magnification using a Zeiss Imager Z1 microscope. Type 1b and 1s boutons were counted using Dlg staining and the number of protrusions and branch points was determined using HRP staining. Confocal images were taken using an LSM 510 META laser scanning microscope (Zeiss). For calculating β-gal signals, maximum projections from z-stacks were analyzed for fluorescence intensity per area with MetaMorph software (Molecular Devices), using DAPI to delineate nuclei. Statistical significance for structural data was determined using a two-tailed Student's t test (Excel). All averages are shown with standard errors. Significant p values are depicted on all bar graphs using the following: * < 0.05, ** < 0.01, *** < 0.005.

SUPPLEMENTAL INFORMATION

Supplemental Information includes four figures and Supplemental Experimental Procedures and can be found with this article online at doi:10.1016/j.neuron.2010.04.011.

ACKNOWLEDGMENTS

We would like to thank G. Bashaw, H. Bellen, L. Luo, J. Ng, H. Keshishian, E. Verheyen, E. Emberly, T. Littleton, A. DiAntonio, N. Lamarche-Vane, and M. O'Connor for reagents and advice. We would like to thank the Bloomington Stock Center for many fly stocks and the Developmental Studies Hybridoma Bank for monoclonal antibodies. We would also like to thank all the members of the Haghighi lab for their support. We are grateful to Corey Goodman for his continuous support of our research program and for providing us with numerous reagents. This work was supported by a fellowship from CIHR and Fragile X Research Foundation to RWB and grants from CIHR, EJLB Foundation, and Genome Canada/Genome Quebec to A.P.H. A.P.H. holds a Tier II Canada Research Chair in Neurobiology.

Accepted: April 2, 2010
Published: May 26, 2010

REFERENCES

Aberle, H., Haghighi, A.P., Fetter, R.D., McCabe, B.D., Magalhães, T.R., and Goodman, C.S. (2002). wishful thinking encodes a BMP type II receptor that regulates synaptic growth in *Drosophila*. Neuron *33*, 545–558.

Albin, S.D., and Davis, G.W. (2004). Coordinating structural and functional synapse development: postsynaptic p21-activated kinase independently specifies glutamate receptor abundance and postsynaptic morphology. J. Neurosci. *24*, 6871–6879.

Awasaki, T., Saito, M., Sone, M., Suzuki, E., Sakai, R., Ito, K., and Hama, C. (2000). The *Drosophila* trio plays an essential role in patterning of axons by regulating their directional extension. Neuron *26*, 119–131.

Bateman, J., and Van Vactor, D. (2001). The Trio family of guanine-nucleotide-exchange factors: regulators of axon guidance. J. Cell Sci. *114*, 1973–1980.

Bateman, J., Shu, H., and Van Vactor, D. (2000). The guanine nucleotide exchange factor trio mediates axonal development in the Drosophila embryo. Neuron *26*, 93–106.

Birch-Machin, I., Gao, S., Huen, D., McGirr, R., White, R.A., and Russell, S. (2005). Genomic analysis of heat-shock factor targets in Drosophila. Genome Biol. *6*, R63.

Bishop, A.L., and Hall, A. (2000). Rho GTPases and their effector proteins. Biochem. J. *348*, 241–255.

Bos, J.L., Rehmann, H., and Wittinghofer, A. (2007). GEFs and GAPs: critical elements in the control of small G proteins. Cell *129*, 865–877.

Brand, A.H., and Perrimon, N. (1993). Targeted gene expression as a means of altering cell fates and generating dominant phenotypes. Development *118*, 401–415.

Briançon-Marjollet, A., Ghogha, A., Nawabi, H., Triki, I., Auziol, C., Fromont, S., Piché, C., Enslen, H., Chebli, K., Cloutier, J.F., et al. (2008). Trio mediates netrin-1-induced Rac1 activation in axon outgrowth and guidance. Mol. Cell. Biol. *28*, 2314–2323.

Bryan, B., Kumar, V., Stafford, L.J., Cai, Y., Wu, G., and Liu, M. (2004). GEFT, a Rho family guanine nucleotide exchange factor, regulates neurite outgrowth and dendritic spine formation. J. Biol. Chem. *279*, 45824–45832.

Budnik, V., Koh, Y.H., Guan, B., Hartmann, B., Hough, C., Woods, D., and Gorczyca, M. (1996). Regulation of synapse structure and function by the *Drosophila* tumor suppressor gene dlg. Neuron *17*, 627–640.

Cingolani, L.A., and Goda, Y. (2008). Actin in action: the interplay between the actin cytoskeleton and synaptic efficacy. Nat. Rev. Neurosci. *9*, 344–356.

Davis, G.W. (2006). Homeostatic control of neural activity: from phenomenology to molecular design. Annu. Rev. Neurosci. *29*, 307–323.

de Curtis, I. (2008). Functions of Rac GTPases during neuronal development. Dev. Neurosci. *30*, 47–58.

Dickson, B.J. (2001). Rho GTPases in growth cone guidance. Curr. Opin. Neurobiol. *11*, 103–110.

Eden, S., Rohatgi, R., Podtelejnikov, A.V., Mann, M., and Kirschner, M.W. (2002). Mechanism of regulation of WAVE1-induced actin nucleation by Rac1 and Nck. Nature *418*, 790–793.

Fan, X., Labrador, J.P., Hing, H., and Bashaw, G.J. (2003). Slit stimulation recruits Dock and Pak to the roundabout receptor and increases Rac activity to regulate axon repulsion at the CNS midline. Neuron *40*, 113–127.

Fanto, M., Weber, U., Strutt, D.I., and Mlodzik, M. (2000). Nuclear signaling by Rac and Rho GTPases is required in the establishment of epithelial planar polarity in the *Drosophila* eye. Curr. Biol. *10*, 979–988.

Fitzsimonds, R.M., and Poo, M.M. (1998). Retrograde signaling in the development and modification of synapses. Physiol. Rev. *78*, 143–170.

Frank, C.A., Pielage, J., and Davis, G.W. (2009). A presynaptic homeostatic signaling system composed of the Eph receptor, ephexin, Cdc42, and CaV2.1 calcium channels. Neuron *61*, 556–569.

Fu, W.Y., Chen, Y., Sahin, M., Zhao, X.S., Shi, L., Bikoff, J.B., Lai, K.O., Yung, W.H., Fu, A.K., Greenberg, M.E., and Ip, N.Y. (2007). Cdk5 regulates EphA4-mediated dendritic spine retraction through an ephexin1-dependent mechanism. Nat. Neurosci. *10*, 67–76.

Galindo, M.I., Bishop, S.A., Greig, S., and Couso, J.P. (2002). Leg patterning driven by proximal-distal interactions and EGFR signaling. Science *297*, 256–259.

Goold, C.P., and Davis, G.W. (2007). The BMP ligand Gbb gates the expression of synaptic homeostasis independent of synaptic growth control. Neuron *56*, 109–123.

Haghighi, A.P., McCabe, B.D., Fetter, R.D., Palmer, J.E., Hom, S., and Goodman, C.S. (2003). Retrograde control of synaptic transmission by postsynaptic CaMKII at the *Drosophila* neuromuscular junction. Neuron *39*, 255–267.

Hakeda-Suzuki, S., Ng, J., Tzu, J., Dietzl, G., Sun, Y., Harms, M., Nardine, T., Luo, L., and Dickson, B.J. (2002). Rac function and regulation during Drosophila development. Nature *416*, 438–442.

Hoodless, P.A., Haerry, T., Abdollah, S., Stapleton, M., O'Connor, M.B., Attisano, L., and Wrana, J.L. (1996). MADR1, a MAD-related protein that functions in BMP2 signaling pathways. Cell *85*, 489–500.

Hu, H., Li, M., Labrador, J.P., McEwen, J., Lai, E.C., Goodman, C.S., and Bashaw, G.J. (2005). Cross GTPase-activating protein (CrossGAP)/Vilse links the Roundabout receptor to Rac to regulate midline repulsion. Proc. Natl. Acad. Sci. USA *102*, 4613–4618.

Innocenti, M., Zucconi, A., Disanza, A., Frittoli, E., Areces, L.B., Steffen, A., Stradal, T.E., Di Fiore, P.P., Carlier, M.F., and Scita, G. (2004). Abi1 is essential for the formation and activation of a WAVE2 signalling complex. Nat. Cell Biol. *6*, 319–327.

Inoue, H., Imamura, T., Ishidou, Y., Takase, M., Udagawa, Y., Oka, Y., Tsuneizumi, K., Tabata, T., Miyazono, K., and Kawabata, M. (1998). Interplay of signal mediators of decapentaplegic (Dpp): molecular characterization of mothers against dpp, Medea, and daughters against dpp. Mol. Biol. Cell *9*, 2145–2156.

Joneson, T., McDonough, M., Bar-Sagi, D., and Van Aelst, L. (1996). RAC regulation of actin polymerization and proliferation by a pathway distinct from Jun kinase. Science *274*, 1374–1376.

Keshishian, H., and Kim, Y.S. (2004). Orchestrating development and function: retrograde BMP signaling in the Drosophila nervous system. Trends Neurosci. *27*, 143–147.

Kuromi, H., and Kidokoro, Y. (2005). Exocytosis and endocytosis of synaptic vesicles and functional roles of vesicle pools: lessons from the Drosophila neuromuscular junction. Neuroscientist *11*, 138–147.

Kusanagi, K., Inoue, H., Ishidou, Y., Mishima, H.K., Kawabata, M., and Miyazono, K. (2000). Characterization of a bone morphogenetic protein-responsive Smad-binding element. Mol. Biol. Cell *11*, 555–565.

Lai, K.O., and Ip, N.Y. (2009). Synapse development and plasticity: roles of ephrin/Eph receptor signaling. Curr. Opin. Neurobiol. *19*, 275–283.

Lin, D.M., and Goodman, C.S. (1994). Ectopic and increased expression of Fasciclin II alters motoneuron growth cone guidance. Neuron *13*, 507–523.

Luo, L. (2000). Rho GTPases in neuronal morphogenesis. Nat. Rev. Neurosci. *1*, 173–180.

Luo, L. (2002). Actin cytoskeleton regulation in neuronal morphogenesis and structural plasticity. Annu. Rev. Cell Dev. Biol. *18*, 601–635.

Luo, L., Liao, Y.J., Jan, L.Y., and Jan, Y.N. (1994). Distinct morphogenetic functions of similar small GTPases: Drosophila Drac1 is involved in axonal outgrowth and myoblast fusion. Genes Dev. *8*, 1787–1802.

Ma, X.M., Huang, J., Wang, Y., Eipper, B.A., and Mains, R.E. (2003). Kalirin, a multifunctional Rho guanine nucleotide exchange factor, is necessary for maintenance of hippocampal pyramidal neuron dendrites and dendritic spines. J. Neurosci. *23*, 10593–10603.

Marqués, G., Bao, H., Haerry, T.E., Shimell, M.J., Duchek, P., Zhang, B., and O'Connor, M.B. (2002). The *Drosophila* BMP type II receptor Wishful Thinking regulates neuromuscular synapse morphology and function. Neuron *33*, 529–543.

Matus, A., Brinkhaus, H., and Wagner, U. (2000). Actin dynamics in dendritic spines: a form of regulated plasticity at excitatory synapses. Hippocampus *10*, 555–560.

McCabe, B.D., Marqués, G., Haghighi, A.P., Fetter, R.D., Crotty, M.L., Haerry, T.E., Goodman, C.S., and O'Connor, M.B. (2003). The BMP homolog Gbb provides a retrograde signal that regulates synaptic growth at the *Drosophila* neuromuscular junction. Neuron *39*, 241–254.

McCabe, B.D., Hom, S., Aberle, H., Fetter, R.D., Marques, G., Haerry, T.E., Wan, H., O'Connor, M.B., Goodman, C.S., and Haghighi, A.P. (2004). Highwire regulates presynaptic BMP signaling essential for synaptic growth. Neuron *41*, 891–905.

Merino, C., Penney, J., González, M., Tsurudome, K., Moujahidine, M., O'Connor, M.B., Verheyen, E.M., and Haghighi, P. (2009). Nemo kinase interacts with Mad to coordinate synaptic growth at the Drosophila neuromuscular junction. J. Cell Biol. *185*, 713–725.

Morales, M., Colicos, M.A., and Goda, Y. (2000). Actin-dependent regulation of neurotransmitter release at central synapses. Neuron *27*, 539–550.

Newsome, T.P., Schmidt, S., Dietzl, G., Keleman, K., Asling, B., Debant, A., and Dickson, B.J. (2000). Trio combines with dock to regulate Pak activity during photoreceptor axon pathfinding in *Drosophila*. Cell *101*, 283–294.

Ng, J., and Luo, L. (2004). Rho GTPases regulate axon growth through convergent and divergent signaling pathways. Neuron *44*, 779–793.

Ng, J., Nardine, T., Harms, M., Tzu, J., Goldstein, A., Sun, Y., Dietzl, G., Dickson, B.J., and Luo, L. (2002). Rac GTPases control axon growth, guidance and branching. Nature *416*, 442–447.

O'Donnell, M., Chance, R.K., and Bashaw, G.J. (2009). Axon growth and guidance: receptor regulation and signal transduction. Annu. Rev. Neurosci. *32*, 383–412.

Osterwalder, T., Yoon, K.S., White, B.H., and Keshishian, H. (2001). A conditional tissue-specific transgene expression system using inducible GAL4. Proc. Natl. Acad. Sci. USA *98*, 12596–12601.

Parnas, D., Haghighi, A.P., Fetter, R.D., Kim, S.W., and Goodman, C.S. (2001). Regulation of postsynaptic structure and protein localization by the Rho-type guanine nucleotide exchange factor dPix. Neuron *32*, 415–424.

Pawson, C., Eaton, B.A., and Davis, G.W. (2008). Formin-dependent synaptic growth: evidence that Dlar signals via Diaphanous to modulate synaptic actin and dynamic pioneer microtubules. J. Neurosci. *28*, 11111–11123.

Penzes, P., Johnson, R.C., Sattler, R., Zhang, X., Huganir, R.L., Kambampati, V., Mains, R.E., and Eipper, B.A. (2001). The neuronal Rho-GEF Kalirin-7 interacts with PDZ domain-containing proteins and regulates dendritic morphogenesis. Neuron *29*, 229–242.

Qurashi, A., Sahin, H.B., Carrera, P., Gautreau, A., Schenck, A., and Giangrande, A. (2007). HSPC300 and its role in neuronal connectivity. Neural Dev. *2*, 18.

Rawson, J.M., Lee, M., Kennedy, E.L., and Selleck, S.B. (2003). Drosophila neuromuscular synapse assembly and function require the TGF-beta type I receptor saxophone and the transcription factor Mad. J. Neurobiol. *55*, 134–150.

Regehr, W.G., Carey, M.R., and Best, A.R. (2009). Activity-dependent regulation of synapses by retrograde messengers. Neuron *63*, 154–170.

Rodal, A.A., Motola-Barnes, R.N., and Littleton, J.T. (2008). Nervous wreck and Cdc42 cooperate to regulate endocytic actin assembly during synaptic growth. J. Neurosci. *28*, 8316–8325.

Sanchez-Soriano, N., Tear, G., Whitington, P., and Prokop, A. (2007). Drosophila as a genetic and cellular model for studies on axonal growth. Neural Dev. *2*, 9.

Schenck, A., Qurashi, A., Carrera, P., Bardoni, B., Diebold, C., Schejter, E., Mandel, J.L., and Giangrande, A. (2004). WAVE/SCAR, a multifunctional complex coordinating different aspects of neuronal connectivity. Dev. Biol. *274*, 260–270.

Schuster, C.M., Davis, G.W., Fetter, R.D., and Goodman, C.S. (1996). Genetic dissection of structural and functional components of synaptic plasticity. I. Fasciclin II controls synaptic stabilization and growth. Neuron *17*, 641–654.

Sekelsky, J.J., Newfeld, S.J., Raftery, L.A., Chartoff, E.H., and Gelbart, W.M. (1995). Genetic characterization and cloning of mothers against dpp, a gene required for decapentaplegic function in Drosophila melanogaster. Genetics *139*, 1347–1358.

Shamah, S.M., Lin, M.Z., Goldberg, J.L., Estrach, S., Sahin, M., Hu, L., Bazalakova, M., Neve, R.L., Corfas, G., Debant, A., and Greenberg, M.E. (2001). EphA receptors regulate growth cone dynamics through the novel guanine nucleotide exchange factor ephexin. Cell *105*, 233–244.

Sone, M., Hoshino, M., Suzuki, E., Kuroda, S., Kaibuchi, K., Nakagoshi, H., Saigo, K., Nabeshima, Y., and Hama, C. (1997). Still life, a protein in synaptic terminals of Drosophila homologous to GDP-GTP exchangers. Science *275*, 543–547.

Sone, M., Suzuki, E., Hoshino, M., Hou, D., Kuromi, H., Fukata, M., Kuroda, S., Kaibuchi, K., Nabeshima, Y., and Hama, C. (2000). Synaptic development is controlled in the periactive zones of Drosophila synapses. Development *127*, 4157–4168.

Steven, R., Kubiseski, T.J., Zheng, H., Kulkarni, S., Mancillas, J., Ruiz Morales, A., Hogue, C.W., Pawson, T., and Culotti, J. (1998). UNC-73 activates the Rac GTPase and is required for cell and growth cone migrations in *C. elegans*. Cell *92*, 785–795.

Stewart, B.A., Atwood, H.L., Renger, J.J., Wang, J., and Wu, C.F. (1994). Improved stability of Drosophila larval neuromuscular preparations in haemolymph-like physiological solutions. J. Comp. Physiol. [A] *175*, 179–191.

Strutt, D.I., Weber, U., and Mlodzik, M. (1997). The role of RhoA in tissue polarity and Frizzled signalling. Nature *387*, 292–295.

Thomas, S., Ritter, B., Verbich, D., Sanson, C., Bourbonnière, L., McKinney, R.A., and McPherson, P.S. (2009). Intersectin regulates dendritic spine development and somatodendritic endocytosis but not synaptic vesicle recycling in hippocampal neurons. J. Biol. Chem. *284*, 12410–12419.

Tolias, K.F., Bikoff, J.B., Kane, C.G., Tolias, C.S., Hu, L., and Greenberg, M.E. (2007). The Rac1 guanine nucleotide exchange factor Tiam1 mediates EphB receptor-dependent dendritic spine development. Proc. Natl. Acad. Sci. USA *104*, 7265–7270.

Twombly, V., Blackman, R.K., Jin, H., Graff, J.M., Padgett, R.W., and Gelbart, W.M. (1996). The TGF-beta signaling pathway is essential for Drosophila oogenesis. Development *122*, 1555–1565.

Twombly, V., Bangi, E., Le, V., Malnic, B., Singer, M.A., and Wharton, K.A. (2009). Functional analysis of saxophone, the Drosophila gene encoding the bmp type I receptor orthologue of human ALK1/ACVRL1 and ACVR1/ALK2. Genetics *183*, 563–579.

Van Aelst, L., and Cline, H.T. (2004). Rho GTPases and activity-dependent dendrite development. Curr. Opin. Neurobiol. *14*, 297–304.

Watabe-Uchida, M., Govek, E.E., and Van Aelst, L. (2006). Regulators of Rho GTPases in neuronal development. J. Neurosci. *26*, 10633–10635.

Wharton, K.A., Cook, J.M., Torres-Schumann, S., de Castro, K., Borod, E., and Phillips, D.A. (1999). Genetic analysis of the bone morphogenetic protein-related gene, gbb, identifies multiple requirements during Drosophila development. Genetics *152*, 629–640.

Yang, L., and Bashaw, G.J. (2006). Son of sevenless directly links the Robo receptor to rac activation to control axon repulsion at the midline. Neuron *52*, 595–607.

Zeng, Y.A., Rahnama, M., Wang, S., Sosu-Sedzorme, W., and Verheyen, E.M. (2007). Drosophila Nemo antagonizes BMP signaling by phosphorylation of Mad and inhibition of its nuclear accumulation. Development *134*, 2061–2071.